

ARTICLES

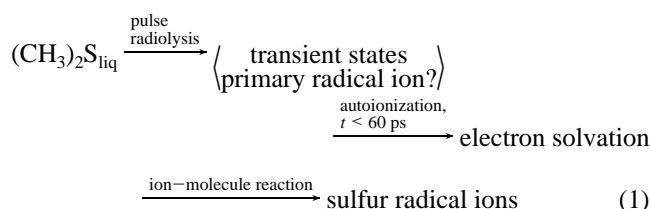
Ultrafast Formation of a Three-Electron-Bonded Radical Anion ($\text{CH}_3\text{S}::\text{SCH}_3^-$) in a Liquid Organic Sulfur CompoundY. Gauduel,^{*,†} J. L. Marignier,[‡] J. Belloni,[‡] and H. Gelabert[†]*Laboratoire d'Optique Appliquée, CNRS URA 1406, INSERM U451, Ecole Polytechnique–ENSTA, 91761 Palaiseau Cedex, France, and Laboratoire de Physico-Chimie des Rayonnements, CNRS URA 75, Université Paris XI, 91405 Orsay, France**Received: June 25, 1997; In Final Form: September 12, 1997*[⊗]

The elementary steps of an electron photodetachment triggered by the UV excitation of pure liquid dimethyl sulfide, $(\text{CH}_3)_2\text{S}$, have been investigated by femtosecond absorption UV–IR spectroscopy at 294 K. The buildup of a long-lived UV band centered around 420 nm (3.26 eV) is observed at the sub-picosecond time scale. This spectral band is assigned to a radical anion ($\text{CH}_3\text{S}::\text{SCH}_3^-$) characterized by a sulfur–sulfur bond with an antibonded third electron (2c, 3e). A very short-lived electronic state, whose rise time equals 180 ± 10 fs, exhibits a spectral overlap with this UV radical. The frequency and time dependences of induced absorption signals are analyzed in the framework of a kinetic model for which an early electron transfer yields an ultrashort-lived anion radical ($\{\text{RSR}^-\}_{\text{RSR}}$ or $\{\text{RSR}::\text{e}^-::\text{RSR}\}$, $\text{R} = \text{CH}_3$). The decay rate of this UV state ($1/\tau = 3.7 \times 10^{12} \text{ s}^{-1}$) is rationalized by postulating an ultrafast ion–molecule reaction and the picosecond formation of a disulfide radical anion ($\text{CH}_3\text{S}::\text{SCH}_3^-$) characterized by a $2\sigma/1\sigma^*$ bond. A second electron-transfer channel leading to a delayed formation of a disulfide anion radical ($\text{RS}::\text{SR}^-$) has been identified by time-resolved IR spectroscopy. These femtosecond investigations argue for an ultrafast formation of a sulfur–sulfur bond with C–S bonds breaking. It is suggested that the density-state fluctuations of organic sulfur molecules influence the energy of early electron–thioether couplings (electron attachment or localization) and would govern competitive branchings between ultrafast electron photodetachment channels.

1. Introduction

Charge-transfer processes involving organic sulfur compounds are of particular interest in biology and chemistry because transient sulfide radical ions can alter or protect the functional properties of enzymatic complexes or proteins.^{1–3} During the past decade, the photochemistry of sulfur-containing molecules has received considerable attention. Research works are mainly devoted to the stabilization of charged sulfides in dilute glass matrixes, the creation of Rydberg series, and state-selected ions in the gas phase by resonantly enhanced multiphoton ionization.^{4–8} Photoexcited organic sulfides undergo different responses which can lead to bond scissions or ionization channels. The primary processes triggered by a UV excitation of liquid organic sulfides correspond to S–S or C–S bond scissions and yield multiple radicals such as methyl thiyl radical ($\text{CH}_3\text{S}^\bullet$ (A)) or thioformaldehyde ($\text{CH}_2\text{S}^\bullet$ (X)).^{9–11} These bond breakings can compete with ultrafast electron photodetachment processes. Indeed, the ionization process can induce a complex radical chemistry including either an electron solvation (e_{sol}^-) or an electron attachment on sulfur molecules with the formation of disulfide anion or cation radicals [$\text{S}::\text{S}]^{\pm,2}$. These radicals characterized by three-electron bonds (2c, 3e⁻) can be produced by ion–molecule reactions.^{12,13} As other radical ions (dihalogen anion radical for instance), they play a significant role in chemistry.^{14,15}

An intriguing case concerns the formation of radical ions in a liquid thioether, dimethyl sulfide (DMS),¹⁶ whose electronic spectrum peaks in the UV.⁹ This organic sulfide ($(\text{CH}_3)_2\text{S}$), represents an important compound in the global sulfur cycle^{17–23} and exhibits different coupling modes with an excess electron. Pulse radiolysis experiments of liquid DMS performed at room temperature have emphasized that both the solvated electron and a secondary anion (RSSR^- , $\text{R} = \text{CH}_3$) are simultaneously identified by their nanosecond spectra.¹⁶ Subnanosecond spectroscopic investigations of pure liquid DMS emphasize that the UV secondary anion (RSSR^-) and the IR solvated electron are totally achieved in less than 60 ps.²⁴ These radiolysis studies argue for the existence of an ultrashort-lived common precursor (a negative adduct) whose behavior would be dependent on a competition between an autoionization process (electron solvation) and an ion–molecule reaction (secondary anionic sulfur radical). Eq 1 summarizes these two hypothetical electron-transfer processes in liquid DMS.



* To whom correspondence should be addressed: Phone: +33(0)1 60 10 03 18. Fax: +33(0)1 60 10 60 85. Email: gauduel@ensta.ensta.fr.

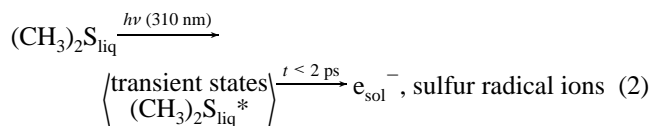
[†] Ecole Polytechnique–ENSTA.

[‡] Université Paris XI.

[⊗] Abstract published in *Advance ACS Abstracts*, November 1, 1997.

Recently, early electron transfers induced by the photoexcitation of liquid DMS have been investigated by sub-picosecond UV–IR spectroscopic techniques.²⁵ At 0.88 eV, an induced

absorption appearing with a time constant of $8 \times 10^{12} \text{ s}^{-1}$ is the signature of a relaxed electron (e_{sol}^-). The discrimination of a UV signal (2.95 eV) in less than $2 \times 10^{-12} \text{ s}$ suggests that ultrafast electron transfers lead to sulfur radical anions and cations (eq 2).



The contribution of a long-lived UV band peaking around 2.95 eV argues for the formation of a sulfur–sulfur radical anion ($\text{RS}\cdot\text{SR}^-$).^{2,16} The energy of this S–S bond characterized by an electronic $2\sigma/1\sigma^*$ configuration is about half of a normal two-electron bond. The low-energy bonding is due to a slight repulsion between two sulfur atoms and involves the effect of two bonding and one antibonding electrons. Disulfide radicals with a three-electron bond (2c, 3e bond) exhibit an absorption UV band peaking around 420 nm.^{12,13,26} Such a band is due to a transition between the uppermost doubly occupied orbital, which represents the σ energy level disturbed by a nonbonding-sulfur electron and the singly occupied σ^* energy level.¹⁵ An energy difference $a_g\{\sigma - n^-\}/b_u(\sigma^*)$ of about 2.5 eV corresponds to an optical transition band centered around 3.5 eV.

The aim of the present work is to investigate one aspect of the time dependence of early electron-transfer branchings in pure liquid DMS. To extend our knowledge of multiple elementary charge-transfer processes, we should address two important questions: (i) Does a transient UV signal characterize a precursor of an anionic radical with a two-center, three-electron sulfur–sulfur bond [$\text{RS}\cdot\text{SR}^-$]? and (ii) does this transient state represent a common precursor for competitive electron solvation and electron attachment? We will mainly focus our attention on the elementary steps that can govern the formation of a 2c, 3e bond within the same temporal regime as an excess electron solvation process. Sub-picosecond UV/IR spectroscopic works have been performed in order to determine whether different electron-transfer trajectories governed by density-state fluctuations of liquid DMS can favor fast or delayed formation of sulfur–sulfur radical anions. These studies are essential for a detailed understanding of radical ion reactivity that will allow one to predict and control the chemistry of sulfur intermediates.

2. Experimental Section

Spectroscopic investigations of ultrafast electron transfer in neat liquid DMS are performed by using a pump–probe configuration with tunable test wavelengths in the UV and near IR (3.26–0.93 eV). Femtosecond pulses centered at 620 nm and as short as 70–80 fs are generated by a passively mode-locked CW dye ring laser (CPM). After amplification, the compression of beams allows output pulses of energy above 10^{-3} J and typically of 80–90 fs duration. One part of the compressed pulses at 620 nm is focused on a KDP crystal for the generation of a second harmonic pump pulse (6–7 μJ at 310 nm, 4 eV), and the other part, on a cell of heavy water (2 cm path length) for the continuum generation (probe beam). After focalization of the UV pump, the power density equals $(6-7) \times 10^{10} \text{ W cm}^{-2}$ in the sample. The test wavelengths selected in the UV (3.66–2.5 eV) and IR ranges (0.93 eV) permit the investigation of transient absorption signals, taking into account the frequency dependence of the instrumental response and several nonlinear optical phenomena (group velocity dispersion, refractive index effect). The zero-time delay is obtained with a time resolution of 20–30 fs in the UV and

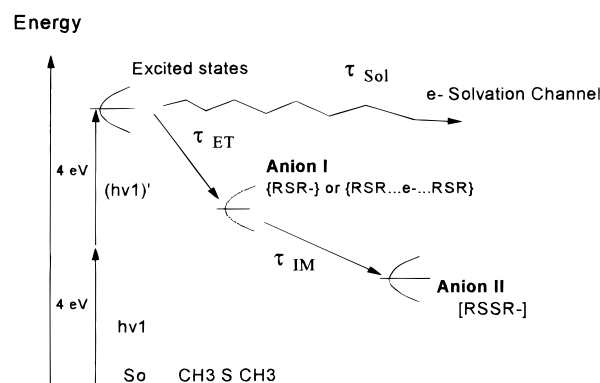


Figure 1. Kinetic model for ultrafast electron transfers in pure liquid dimethyl sulfide ($(\text{CH}_3)_2\text{S}$). This model considers a branching between an electron solvation process and the formation of primary sulfur radical anions (anion I, anion II).

IR. The details of the spectroscopic procedures within a large spectral range ($26\,000\text{--}7500 \text{ cm}^{-1}$) have been published in recent papers.²⁷ Data acquisition is through custom software written in Fortran and C^{++} . Each data point represents the average of 2000 laser shots, and a time-resolved curve is defined by typically 100 points.

DMS is obtained from Aldrich as 99.99% grade. Its ultimate purification over sodium and transfer distillation under vacuum into the experimental cell has been previously described.^{24,25} The optical density of the cell at the pump wavelength (310 nm) equals 0.034 at 294 K. The experiments were performed in a continuously vibrating fixed volume Suprasil cell equipped with an expansion volume ($\sim 2 \text{ mL}$) so that each amplified laser pulse excites a new region of the sample.

3. Results and Discussion

3.1. Femtosecond UV Spectroscopy of Primary Anionic Radicals. The UV excitation of neat liquid DMS with femtosecond 310 nm pulses (4 eV) has been performed outside the long-wavelength absorption edge of the DMS absorption band centered at 210 nm. The electronic transition linked to the lowest energy tail of the UV absorption band of liquid DMS exhibits a $4s \leftarrow 3p$ character.⁹ Although the ionization potential of liquid DMS is unknown, it is lower than the ionization potential (8.65 eV) in the gas phase.^{28,29} Preliminary femtosecond spectroscopic investigations have shown that the photoexcitation of neat liquid DMS with intense UV pulses ($\sim 10^{10} \text{ W cm}^{-2}$) leads to an efficient electron photodetachment within the first 500 fs after the energy deposition.²⁵ Due to the high-energy power of the UV pulses, a two-photon ionization process with UV femtosecond pulses has been previously observed in polar solutions and nonpolar liquids.³⁰ In the present work, if the femtosecond photoionization of $(\text{CH}_3)_2\text{S}$ molecules is induced by a two-photon absorption process, the energy deposition would correspond to 8 eV (Figure 1). To limit the contribution of a higher nonlinear process, the intensity of the pump pulse is limited to the energy range 5.5–7 μJ . The energy level of 8 eV ($2 \times 4 \text{ eV}$) being higher than the supposed vertical ionization threshold or the measured photolysis threshold (195 nm, 6.35 eV), the excited DMS molecules should be ionized and/or dissociated.¹⁰ The fact that a DMS sample exhibits a very small absorption at 310 nm ($\text{OD} = 0.017$ for $l = 1 \text{ mm}$) does not permit the exclusion of the contribution of a one-photon excitation process with a vertical transition of 4 eV. Regarding the very small transient UV signal obtained following the femtosecond UV excitation ($t \approx 500 \text{ fs}$), it is very difficult to determine the respective contributions of the mono- and biphotonic absorption processes because the early branching

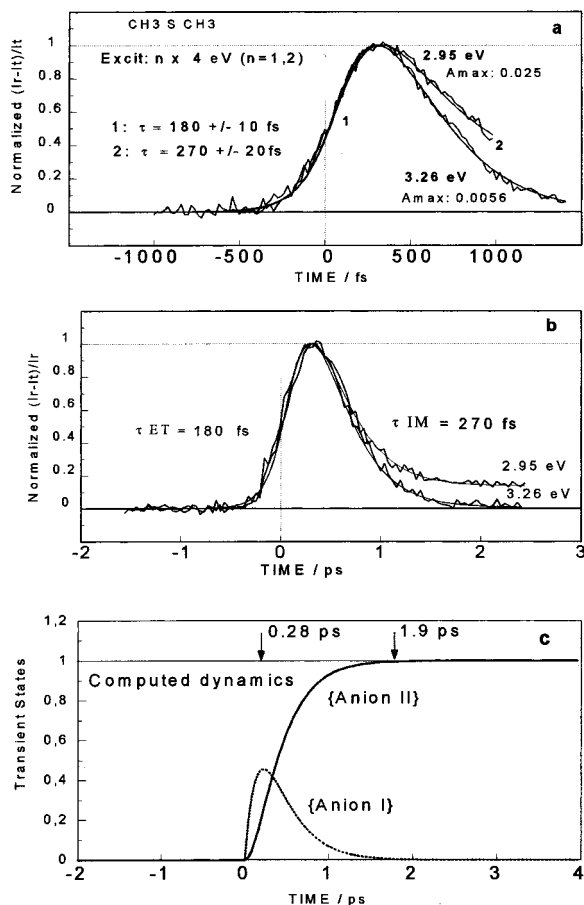


Figure 2. Short-time dependence of induced absorption signals at 3.26 and 2.95 eV following the femtosecond UV excitation of pure dimethyl sulfide at 294 K. The transient signal observed at 3.26 eV (380 nm) represents the contribution of a very short-lived primary radical anion whose deactivation rate (τ_{IM}) equals $3.3 \times 10^{12} \text{ s}^{-1}$. At 2.95 eV (420 nm), the incomplete recovery of the transient absorption signal is assigned to a long-lived radical anion with a sulfur–sulfur bond ($\text{CH}_3\text{S}\cdot\text{SCH}_3^-$). Part c of the figure represents the computed time dependence of a primary (anion I) and secondary radical anion (anion II). These elementary electron transfers are achieved in less than $2 \times 10^{12} \text{ s}^{-1}$.

ratio between multiple primary photochemical processes cannot be directly measured. The time dependence of two photoinduced UV absorption data obtained at 3.26 and 2.95 eV is reported in Figure 2. These transient signals are characterized by a very small amplitude ($\Delta_{OD} \approx 0.0056\text{--}0.025$) and the presence of an ultrashort-lived component whose relaxation is totally achieved in less than 2 ps. Moreover, the contribution of a long-lived electronic state is also observed within the spectral range 3.26–2.48 eV (Figure 3). The photoinduced absorption signals are analyzed with a numerical model which considers the time or frequency dependence of early photo-physical steps.

Femtosecond Kinetic Model of Transient Electronic States.

For a given probe wavelength ω_T , the time dependence of an induced absorption signal $S^{\omega_T}(\tau)$ is expressed by the physical response “ R ” of the sample and the normalized correlation function between the excitation pulse (I_P) and the probe beam (I_T) separated by a time delay τ . This correlation function is dependent on the pump–probe pulse duration, the propagation of the pump–probe pulses, and the overall optical broadening factor due to the group velocity dispersion within the DMS sample (eq 3).

$$S^{\omega_T}(\tau) = (R \otimes \{I_P^n \otimes I_T\})(\tau) \quad (3)$$

The propagation of a pump beam along the z axis in the thioether DMS sample is dependent on the transition $n_i \Rightarrow n_j$ triggered by one- or two-photon interactions:³¹

$$\frac{\partial}{\partial z'} I_P(z', t') = - \sum_{i < j} \sigma_{ij}(\omega_P) \{n_i(z', t') - n_j(z', t')\} I_P(z', t') - \beta(\omega_P, \omega_P) I_P^2(z', t') \quad (4)$$

In this expression, σ_{ij} represents the absorption cross section of the transition $n_i \Rightarrow n_j$, and the time dependence of the state i is defined by the differential equation

$$\frac{\partial}{\partial t'} n_i(z', t') = -\alpha(\omega_P, z', t') \frac{I_P(z', t')}{\hbar \omega_P} - \beta(\omega_P, \omega_P) \frac{I_P^2(z', t')}{2\hbar \omega_P} + \sum_i \left(\frac{n_j(z', t')}{\tau_{ji}} - \frac{n_i(z', t')}{\tau_{ij}} \right) \quad (5)$$

The propagation of the probe beam (I_T) in the sample is defined by the relation

$$\frac{\partial}{\partial z''} I_T(z'', t'') = -\beta^*(\omega_P, \omega_T) I_P\left(z'', t'' + \frac{z''}{\Delta}\right) I_T(z'', t'') - \sum_{i < j} \sigma_{ij}(\omega_T) \left(n_i\left(z'', t'' + \frac{z''}{\Delta}\right) - n_j\left(z'', t'' + \frac{z''}{\Delta}\right) \right) I_T(z'', t'') \quad (6)$$

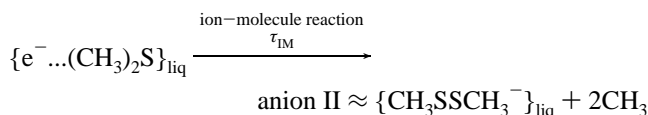
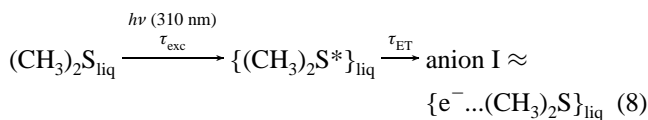
In expression 6,

$$t'' = t' - z'/\Delta, \quad z' = z'', \quad \frac{1}{\Delta} = \frac{1}{v_T} - \frac{1}{v_P}$$

The induced absorption signal triggered by the pump and measured by the probe beam is expressed by the following equation:

$$D(t'') = 1/2.3 \left\{ \int_{z''=0}^{z''=x} \left[\beta^*(\omega_P, \omega_T) I_P\left(z'', t'' + \frac{z''}{\Delta}\right) I_T(z'', t'') + \sum_{i < j} \sigma_{ij}(\omega_T) \left(n_i\left(z'', t'' + \frac{z''}{\Delta}\right) - n_j\left(z'', t'' + \frac{z''}{\Delta}\right) \right) \right] dz'' \right\} \quad (7)$$

The elementary steps of an electron attachment occurring from excited DMS molecules are described by a two-state model (Figure 1, eq 8) and two differential equations (eqs 9, 10). The two-state model considers an ultrafast electron photodetachment and a subsequent electron attachment on adjacent organic molecules. This channel would lead to the a primary ion radical (anion I). The second step yields a long-lived anion (anion II).



These two elementary electron-transfer steps (primary anion formation and anion stabilization) are expressed by differential equations:

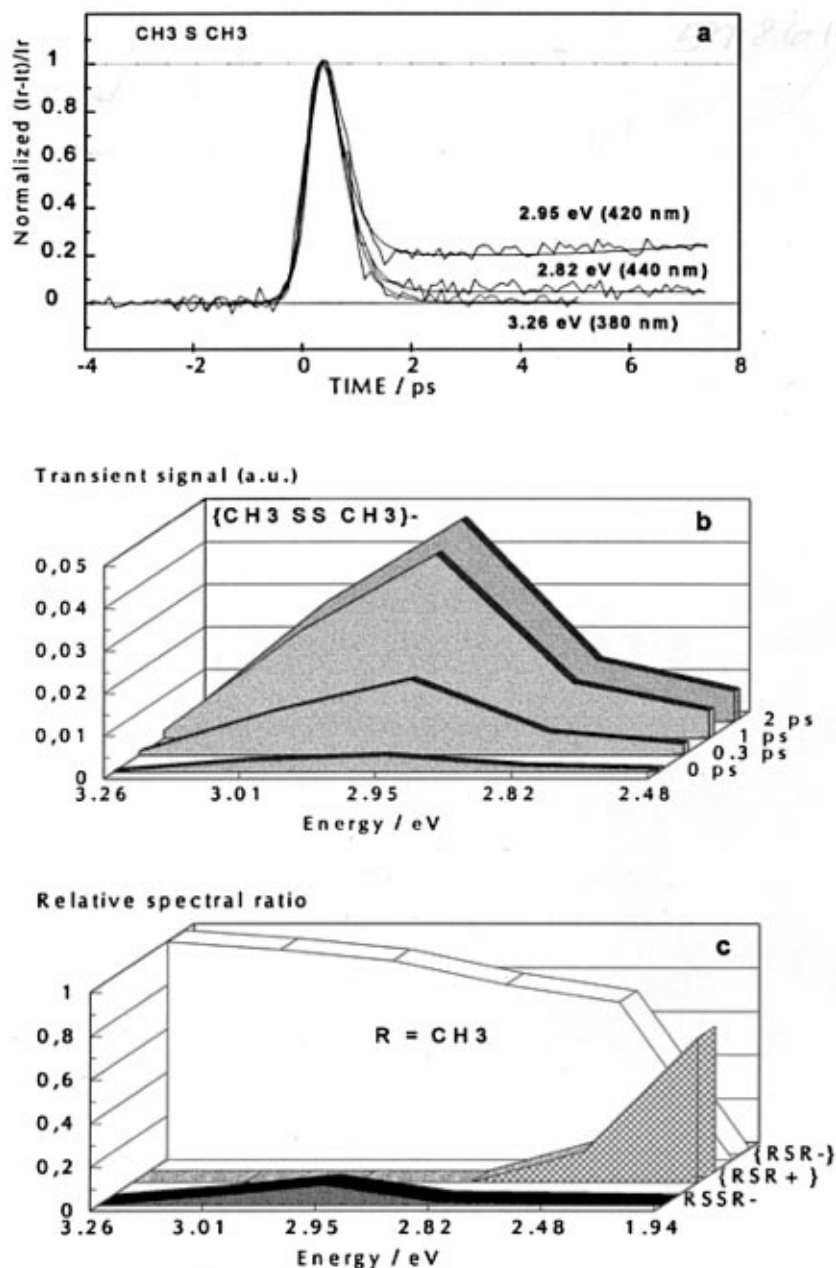


Figure 3. (a) Set of experimental UV spectroscopic curves following the UV femtosecond excitation of liquid DMS at 294 K. (b) Calculated optical absorption of a secondary sulfur–sulfur radical $[\text{CH}_3\text{S}\cdot\text{SCH}_3]^-$. The relative spectral contributions of anionic and cationic sulfur radicals ($\text{CH}_3\text{SCH}_3^-$, $\text{CH}_3\text{SCH}_3^+$, $\text{CH}_3\text{S}\cdot\text{SCH}_3^-$) are shown in part c of the figure.

Ultrafast electron photodetachment and formation of a primary anion {anion I}:

$$\frac{\partial n_{\text{anion I}}(t)}{\partial t} = \frac{n_{\text{RSR}}^{*(t)}}{\tau_{\text{ET}}} - \frac{n_{\text{anion I}}(t)}{\tau_{\text{IM}}} \quad (9)$$

Ultrafast anion–molecule reaction and formation of a secondary anion {anion II}:

$$\frac{\partial n_{\text{anion II}}(t)}{\partial t} = \frac{n_{\text{anion I}}(t)}{\tau_{\text{IM}}} \quad (10)$$

As shown in Figure 1, the transient UV state (anion I) would correspond to an intermediate step of an anionic radical stabilization (anion II). One of the key points we have investigated at different temporal windows (2, 4, and 6 ps) concerns the time dependence of the UV transient contribution (τ_{ET} , τ_{IM}). From best computed fits, we can extract the energy

dependence of adjusted parameters linked to short- and long-lived components. The time dependence of the measured absorption signal $S^{\omega\text{T}}(\tau)$ can be defined by expression 11.

$$S^{\omega}(\tau) = \sum_i \{ \alpha_i^{\omega} \int_{-\infty}^{+\infty} n_i(t-\tau) \otimes \text{Corr}^{\omega\text{p},\omega\text{T}}(t) dt \} \quad (11)$$

$\text{Corr}^{\omega\text{p},\omega\text{T}}$ is the correlation function between the excitation and test beams.²⁷

The best computed fits of UV signals (3.26–2.82 eV) are obtained with a linear combination of two spectral contributions (eqs 12, 13). The relative contributions of transient radical anions are determined from normalized absorption signals. The coefficients $\alpha_1^{\omega\text{T}}$, $\alpha_2^{\omega\text{T}}$ are defined in expression 13:

$$\Delta A^{\omega\text{T}}(\tau) = \Delta A^{\omega\text{T}}_{\text{anion I}}(\tau) + \Delta A^{\omega\text{T}}_{\text{anion II}}(\tau) \quad (12)$$

with

$$\Delta A^{\omega T}(\tau) = \alpha_1^{\omega T}[\text{anion I}](\tau) + \alpha_2^{\omega T}[\text{anion II}](\tau) \quad (13)$$

These expressions take into account the time dependence of the transient sulfur anionic radicals. At a given probe wavelength, the adjusted parameters $\alpha_1^{\omega T}$, $\alpha_2^{\omega T}$ represent the relative spectral contribution of anion I and anion II, respectively. When the computed analyses are performed from normalized signals ($S^{\omega T}_{\text{nor}}(\tau)$), expression 11 becomes

$$S^{\omega T}_{\text{nor}}(\tau) = \sum_i \alpha_i^{\omega T} n_i(\tau) / \sum_i \alpha_i^{\omega T} n_i(\tau S_{\text{max}}) \quad (14)$$

The normalization factors used in expression 14 require that $\sum_i \alpha_i^{\omega T} = 1$.

To maintain the consistency of our kinetic model, two adjusted temporal parameters (τ_{ET} , τ_{IM}) have been analyzed for different temporal windows (2, 4, 6 ps) and probe wavelengths (380–500 nm, i.e., 3.26–2.48 eV). From computed analysis of normalized experimental curves, it is possible to determine (i) the dynamics of the two electronic states (Anion I, Anion II) and (ii) the spectral contribution of sulfur anion radicals.

Spectral Identification of Primary Anionic Sulfur Radicals. At 3.26 and 2.95 eV (360 and 420 nm) the best computed fits of induced UV absorption data yield a rise time (τ_{ET}) of 180 ± 10 fs (Figure 2). Compared to the instrumental response, this ultrashort-lived UV component does not correspond to an instantaneous signal rise time and cannot be assigned to a direct formation of excited DMS molecules or photoproducts triggered by a vertical transition within a Born–Oppenheimer approximation. The numerical analysis of this transient UV signal yields a monoexponential relaxation whose time constant τ_{IM} equals 270 ± 20 at 3.26 or 2.95 eV (Figures 1, 2).

At this stage of the analysis, we explored whether the relaxation of this transient UV state leads to the formation of a long-lived sulfur–sulfur radical anion (eq 8). The main results are reported in Figures 2 and 3. At 3.26 eV (380 nm), the spectral contribution of a long-lived component remains negligible and represents less than 0.1% of the transient UV signal. Scanning with the femtosecond test wavelength, the frequency dependence of the incomplete UV signal recovery was determined. A contribution of a long-lived electronic state can be observed between 380 and 500 nm (Figure 3a, b, or c). The time and wavelength dependence of incomplete UV signal recovery are well featured by the two-state model for which two electronic states are considered (anions I, II). The computed time dependence of these anion sulfur radicals is reported in Figure 2c. According to eqs 8–10, the sub-picosecond signature of the secondary anionic radical (anion II) is largely governed by the relaxation rate of the primary anion (anion I). Consequently, the time dependence of this secondary radical is defined by the following expression:

$$\text{anion II}(t) = A^0 \{ 1 - 1/(\tau_{\text{IM}} - \tau_{\text{ET}}) [\tau_{\text{IM}} \exp(-t/\tau_{\text{IM}}) - \tau_{\text{ET}} \exp(-t/\tau_{\text{ET}})] \} \quad (15)$$

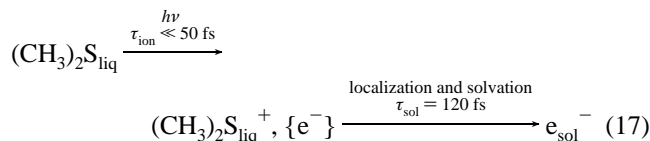
For a time delay τ defined between 0 and +2 ps, the spectrum buildup of the long-lived sulfur radical (anion II) is expressed by the relation

$$S^{\omega T}_{\text{anion II}}(\tau) = \alpha^{\omega T}_{\text{anion II}} n_{\text{anion II}}(\tau) \quad (16)$$

Under our experimental conditions, an UV band centered around 2.95 eV (Figure 3) is fully developed in less than 2 ps after the energy deposition (Figure 2). The lower part of Figure 2 shows the absolute time dependence of two electronic states which contribute to UV signals. Considering previous quantum

calculations on anionic sulfur radicals in solutions,^{2,15} the position of our calculated UV band (420 nm) at $\tau = +2$ ps argues for an early existence of a sulfur–sulfur anionic radical ($\text{CH}_3\text{S}\cdot\text{SCH}_3^-$) characterized by an electronic $2\sigma/1\sigma^*$ configuration (2c, 3e bond). Moreover, the localization of this early UV band agrees with pulse radiolysis experiments on pure liquid DMS²⁴ or organic sulfur solutions^{2,32} and for which a sub-nanosecond UV band peaking at 420 nm has been assigned to the disulfur radical anion (anion II or RSSR^-). In the present work, the calculated spectrum of the sulfur–sulfur anionic radical is in agreement with femtosecond spectroscopic investigations using an optical multichannel analyzer (OMA IV) equipped with a cooled CCD detector.³³

The sub-picosecond identification of an UV anion radical emphasizes that the femtosecond excitation of pure DMS initiates ultrafast electron transfers. Femtosecond UV and IR spectroscopic investigations of electronic dynamics in pure liquid DMS allow us to identify two well-defined ultrafast electron-transfer processes which are totally achieved within $2 \times 10^{12} \text{ s}^{-1}$ (Figures 3, 4). The existence of an ultrafast photoionization channel triggered by femtosecond UV excitation of liquid DMS has been established by IR spectroscopy²⁵ and is confirmed by visible spectroscopic data (Figure 3). For the first time, the signature of a highly reactive cation (RSR^+) has been identified in the red spectral region. The “instantaneous” rise of this excited sulfur cation occurs within the pump–probe correlation function, and its deactivation rate equals $1.11 \times 10^{12} \text{ s}^{-1}$ at 294 K.³³ The photoionization channel involves also an electron solvation process whose time constant equals 120 ± 20 fs at 0.93 eV (eq 17). This IR solvated electron exhibits a high mobility coefficient and an efficient coupling with aromatic acceptors such as biphenyl.^{23,25}



On the other hand, regarding the femtosecond UV spectroscopic data (eqs 8, 12, 13), we tentatively conclude the existence of an ultrafast electron-transfer trajectory in which a very short-lived intermediate (anion I) represents a direct precursor of the long-lived sulfur–sulfur radical anion (anion II). The decay of this primary anion has been analyzed in the framework of an ultrafast ion–molecule process. The high deactivation rate of eq 8 ($3.7 \times 10^{12} \text{ s}^{-1}$) suggests an efficient p orbital overlap between two interacting sulfur atoms and a high cross section for the interaction of the unbound electron (σ^* antibonded third electron) with a newly established σ sulfur–sulfur bond. The time-resolved results reported in the lower part of Figure 4 permit a comparison between the IR electron localization dynamics and the UV disulfide anion radical formation. These two electron-transfer trajectories occur at the sub-picosecond time scale, but the electron solvation process is achieved before the ion–molecule reaction. The measured time delay of about 800 fs can be indicative of a specific molecular response of DMS molecules following a charge redistribution within the newly formed disulfide anion radical (anion II). This molecular response would involve a C–S bond breaking (methyl abstraction) and an intramolecular stabilization of the three-electron bond. This time delay is not observed when the UV disulfide anion radical is initiated by a direct electron attachment of a p-like state on a S–S bond.³³

3.2. UV/IR Spectroscopy of a Delayed Electron Attachment. Femtosecond IR and UV spectroscopy of liquid DMS

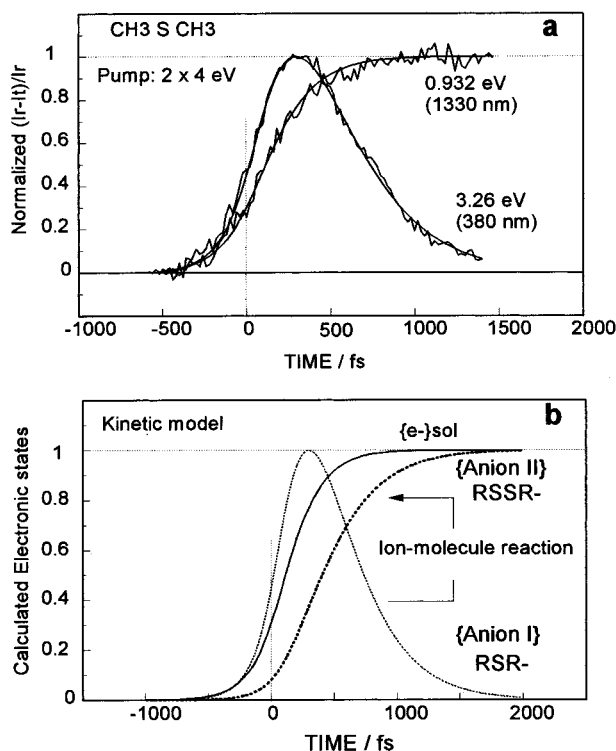
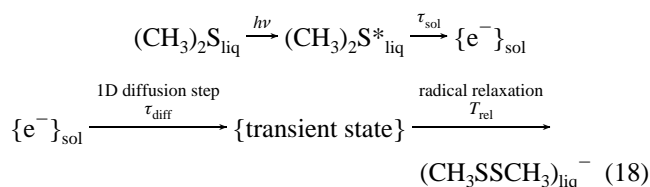


Figure 4. Time dependence of two electron-transfer trajectories following the femtosecond UV photoionization of neat liquid CH_3SCH_3 at 294 K. The smooth lines represent the best computed fits of UV and IR spectroscopic data. The IR signal rise time at 0.932 eV occurs with a characteristic time constant of 120 ± 20 fs. This electronic dynamics is assigned to an electron solvation process (e_{sol}^-). Part b of the figure compares the dynamics of two electron-transfer processes: an IR electron solvation and a direct electron attachment on $(\text{CH}_3)_2\text{S}$ molecules (eqs 8, 17).

permits us to push ahead the understanding of ultrafast electron-transfer branchings in liquid organic sulfurs. The results reported in Figures 5 and 6 show that the infrared absorption signal assigned to fully relaxed electrons exhibits a nonexponential decay. This dynamical behavior is assigned to the reactivity of an electron ground state with thioether molecules. From the photophysical point of view, we should wonder whether this electron transfer corresponds to a slow electron attachment on DMS molecules with the delayed formation of sulfur anion radicals. Equation 18 reports the early electron-transfer steps considered at the picosecond time scale:



The high mobility of localized electrons in thioether DMS¹⁶ would favor efficient scattering events through a density-state fluctuations profile. The computed analysis of IR signals considers a diffusive 1D trajectory. The differential equation of this isotropic process is given from the second Fick law:

$$\frac{\partial}{\partial t} C(x,t) = D \frac{\partial^2 C}{\partial x^2} \quad (19)$$

The analytic solution of a unidirectional diffusion model is given by the expression

$$C(x,t) = (C^0/2\sqrt{Dt\pi}) \text{erf}(x/2\sqrt{Dt}) \quad (20)$$

The time dependence of the IR solvated electrons level $\{\text{e}^-\}_{\text{sol}}$ is expressed by the differential equation

$$\frac{\partial}{\partial t} n_{\text{e}_{\text{sol}}^-}(t) = \frac{n_{\text{RSR}^*}(t)}{\tau_{\text{sol}}} - \varphi n_{\text{e}_{\text{sol}}^-}(t) \left(\frac{\partial}{\partial t} \text{erf} \sqrt{\frac{\tau_{\text{diff}}}{t}} \right) \quad (21)$$

In this equation, τ_{diff} represents the time dependence of a finite 1D electron transfer, φ the fraction of IR solvated electrons involved in a unidirectional diffusion process, and τ_{sol} the solvation time of an excess electron in liquid DMS. The best computed fits of IR spectroscopic data obtained between 2 and 100 ps are reported in Figures 4 and 5. The frequency ($1/\tau_{\text{diff}}$) of the 1D electron-transfer trajectory equals $0.52 \times 10^{11} \text{ s}^{-1}$ at 294 K, and the fraction of electron ground state (φ) linked to this process equals 0.67 ± 0.03 (Figure 5). It is interesting to underline that the extrapolation of this IR analysis to the subnanosecond regime (0.5–2.5 ns) permits us to estimate the time dependence of IR solvated electrons in DMS. Figure 5 predicts the contribution of an early signal decay ($\sim 50\%$) within the first 500 ps after the energy deposition. At longer time, a monotonic influence of the 1D diffusion process is more likely. In agreement with previous pulse radiolysis works,²⁵ the ground state of photodetached electrons would exhibit a detectable subnanosecond IR signature. However, the long-lived contribution of solvated electrons in DMS would represent less than 40% of the initial level of photodetached electrons. The analysis of UV signal dynamics is reported in Figure 6. Computed fits of time-resolved IR and UV data suggest the existence of a picosecond 1D electron-transfer channel yielding a second UV anionic sulfide radical (eqs 18, 21, 22).

$$\frac{\partial}{\partial t} n_{\text{transient state}}(t) = \varphi n_{\text{e}_{\text{sol}}^-}(t) \left(\frac{\partial}{\partial t} \text{erf} \sqrt{\frac{\tau_{\text{diff}}}{t}} \right) - \frac{n_{\text{transient state}}(t)}{\tau_{\text{rel}}} \quad (22)$$

$$\frac{\partial}{\partial t} n_{(\text{CH}_3\text{SSCH}_3)^-}(t) = \frac{n_{\text{transient state}}(t)}{\tau_{\text{rel}}} \quad (23)$$

In this photochemical channel, the 1D limiting step would correspond to an electron ground-state transfer characterized by the time constant τ_{diff} (delayed electron attachment on DMS configurations). The time dependence of the transient state (eq 22) is controlled by a slow 1D step and an ultrafast reorganization of the thioether molecules in order to favor the stabilization of anionic sulfur radicals (ultrafast ion–molecule reaction). Consequently, the time dependence of the UV signature of $\text{S}-\text{S}^-$ is expressed by eq 23, in which τ_{rel} represents the dynamics of an ultrafast ion–molecule process. Figure 6 demonstrates that the signal rise time observed at 2.95 eV (420 nm) is well-defined by the differential equations (21, 22). In this kinetic model, τ_{diff} (19 ps) is determined by IR spectroscopy (Figure 5) and $1/\tau_{\text{rel}}$ is equivalent to $1/\tau_{\text{IM}}$ ($3.7 \times 10^{12} \text{ s}^{-1}$). The UV signal rise time analysis is performed within a spectral range for which the contribution of a sulfur–sulfur radical anion ($\text{CH}_3\text{S}^{\cdot-}:\text{SCH}_3^-$) with a $2\sigma/1\sigma^*$ bond radical is maximum (Figures 3, 6). The picosecond spectral signature observed at 2.95 eV is attributed to a diffusion-controlled formation of the $\text{S}-\text{S}^-$ radical from the IR ground state of the solvated electron (eq 18). This reasonable conclusion is maintained from convergent UV/IR spectroscopy of transient and stabilized electronic states in DMS (eq 18). The computed IR dynamics emphasize that an early relaxation is mainly governed by a 1D diffusional process of the solvated ground state (Figure 5). This

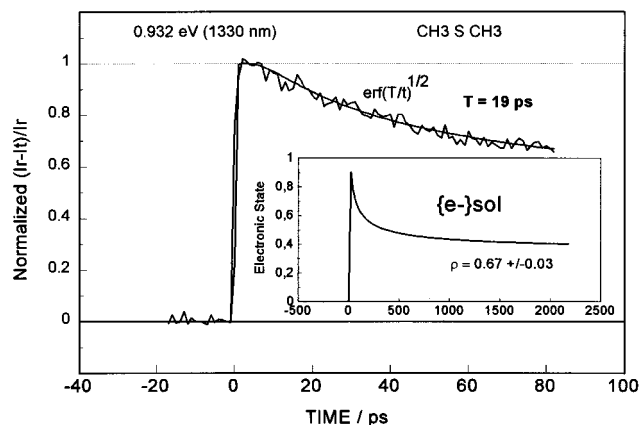


Figure 5. Sub-nanosecond electron-transfer dynamics in neat liquid $(\text{CH}_3)_2\text{S}$ at 294 K. This delayed electron-transfer process involves 67% of an initial population of relaxed electrons (ground state of solvated electron) and yields a second population of disulfur radical anions. For explanations see eqs 18–23.

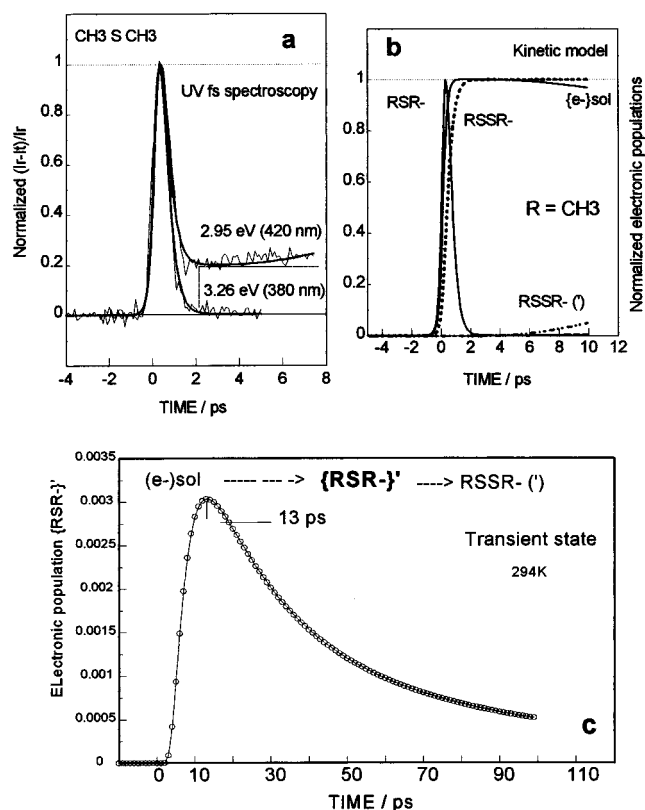


Figure 6. Time-resolved spectroscopy of a delayed electron-transfer process in liquid $(\text{CH}_3)_2\text{S}$ (a, b). This charge transfer corresponds to a second formation channel of a sulfur–sulfur radical anion $[\text{CH}_3\text{S}\cdot\cdot\text{SCH}_3]^-$. A transient state of this delayed electron attachment process (eq 18) would exhibit a maximum around 13 ps (c).

dynamics agrees with the UV signal rise time due to a second RSSR^- radical formation pathway noted $\text{RSSR}^{-(\prime)}$ in Figure 6. The calculated dynamics of the transient state involved in this delayed electron attachment (an unstable anionic sulfur radical, $\text{RSR}^{-(\prime)}$) shows a contribution maxima around 13 ps. The very low concentration of this transient state cannot be directly discriminated by femtosecond UV spectroscopy.

4. General Discussion and Conclusions

The femtosecond UV–IR spectroscopy of liquid DMS provides direct evidence of ultrafast electron transfers (Figure 7) whose fully relaxed states have been previously observed.^{23–25}

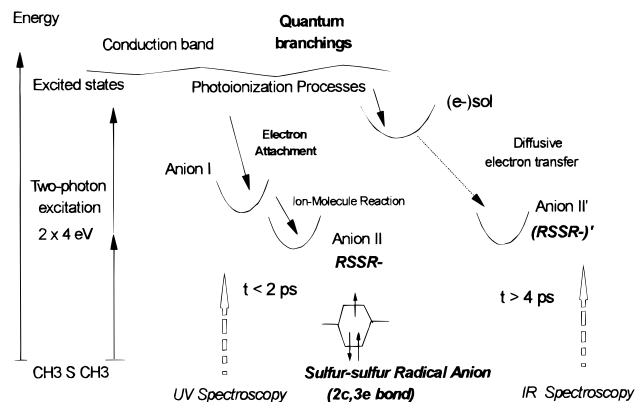


Figure 7. Scheme of primary electron-transfer trajectories triggered by an UV photoexcitation of DMS molecules. The first ultrafast channel implies a direct electron attachment on thioether molecules (monomer or dimer configurations). A very short-lived UV intermediate is assigned to a primary radical anion (anion I). This state involves an ion–molecule reaction and the sub-picosecond formation of an anionic radical with a two-center, three-electron sulfur–sulfur bond (anion II: $[\text{CH}_3\text{S}\cdot\cdot\text{SCH}_3]^-$). The second trajectory corresponds to an electron detachment and a subsequent electron solvation process. A significant fraction of this channel ($\rho \approx 67\%$) is followed by a diffusive 1D electron attachment and yields a second formation channel of anion II', $\text{R} = \text{CH}_3$. The time dependence of these elementary charge transfers has been investigated by UV and IR spectroscopy (Figures 4–6).

One of the key points of this work concerns the UV identification of a very short-lived precursor of a S–S three-electron-bonded radical anion $[\text{CH}_3\text{S}\cdot\cdot\text{SCH}_3]^-$. From the energy point of view, the identification of the UV state in less than 300 fs cannot be considered as a direct precursor of IR solvated electrons. The deactivation rate of this UV state ($3.7 \times 10^{12} \text{ s}^{-1}$) is rather rationalized by postulating ultrafast ion–molecule reactions and the disulfide anion radical formation $[\text{RS}\cdot\cdot\text{SR}^-]$ in less than 2 ps. The ultrafast formation of a SS^- bond ($2\sigma/1\sigma^*$ bond) whose strength is in the range 40–120 kJ/mol¹⁵ raises a fundamental question about the eigenstate of an unpaired electron within short-lived primary anions. The transient anion radical (anion I) can be understood either as a direct electron attachment on a monomer (RSR^-) or as a more complicated resonance coupling with preexisting sulfur complexes ($\text{RSR}\cdot\cdot\text{e}^- \cdot\cdot\text{RSR}$). Does this electron correspond to an s-like or p-like orbital? If the transient precursor of $\text{CH}_3\text{S}\cdot\cdot\text{SCH}_3^-$ is equivalent to an anionic monomer, its deactivation frequency would involve a significant reorganization of surrounding molecules. The ultrafast stabilization of a disulfide radical anion raises the role of complex electronic and molecular processes linked to the internuclear distance of the S atom, the favorable angular orientation of the interacting p orbitals for an efficient orbital overlap, the participation of a directed orbital (p orbital) or undirected orbital (s orbital) of the third electron, an efficient concerted S–C bond breaking (demethylation process), and a solvent relaxation around the newly established radical anion. The femtosecond investigations of $\text{CH}_3\text{S}\cdot\cdot\text{SCH}_3^-$ do not permit obtaining good accuracy of the optical absorption maxima position. However, the computed UV band centered around 420 nm (2.95 eV) seems slightly red-shifted by comparison with the sub-microsecond band peaking at 407 nm (3.05 eV).²⁶ Regarding the time dependence of this UV band, we should wonder whether (i) this initial red-shift ($\sim 0.095 \text{ eV}$) means an incomplete relaxation of the secondary radical anion and (ii) a long time solvent contribution assists the stabilization of the sulfur–sulfur bond with an antibonded third electron.

An important point raised by this study is that the formation dynamics of a disulfide radical anion $[\text{RS}\cdot\cdot\text{SR}^-]$ with a σ^* antibonded third electron is slower than the electron solvation

process. The formation of an excess electron by ionization leads to an ultrafast IR solvation process in less than 1 ps at 294 K. This solvation dynamics is faster than the electron hydration process but remains similar to an electron localization dynamics in a liquid hydrocarbon.³⁰ Contrary to previous conclusions raised from pulse radiolysis investigation of this thioether,^{16,24} the present work does not permit emphasizing the existence of a common precursor (anionic monomer of DMS) whose ultrafast relaxation would involve either an electron solvation or an ion–molecule reaction (disulfide anion radical formation). The identification of two ultrafast electron transfers suggests the existence of a still earlier statistical energy partitioning due to the density-state fluctuations of the liquid thioether. Therefore we conclude that the electron solvation and the disulfide anion radical formation proceed through two independent electron photodetachment processes. Further spectroscopic works would permit extending our understanding on quantum branchings of electron transfer and on the role of electronic and molecular dynamics during the formation of sulfur-centered three-electron-bonded radicals [RS·SR⁻]. The electron ground state (e_{sol}⁻) exhibits a long-lived component in the nanosecond regime, but a non-negligible fraction ($\varphi = 0.67 \pm 0.03$) participates in the picosecond stabilization of a disulfide anion radical. Within the 10–100 ps after the initial energy deposition, this “slow” electron-transfer mechanism is understood as a diffusive 1D electron attachment on DMS molecules (eq 18) and yields an UV absorbing sulfur–sulfur radical anion with a $2\sigma/1\sigma^*$ bond.

Highly time-resolved spectroscopic works are in progress in order to assess the influence of early anisotropic electron–DMS couplings during the formation of a disulfide radical anion. It would be fundamental to investigate the influence of an excess electron eigenstate on the torsional potential functions of DMS molecules and the nature of transient couplings between an electron and the potential energy surface of the methyl rotation monomers. In the gas phase, two internal C_{3v} rotors have been observed,³⁴ and the intramolecular interaction between the methyl groups is normally slightly repulsive.³⁵ The direct characterization of ultrashort-lived electronic states in liquid DMS provides a further basis for the microscopic investigations of elementary sulfur radical reactions triggered by the oxidation or the reduction of organic sulfides.^{2,36–40} The understanding of transient states that involve an interaction between an excess electron and DMS molecules represents a many-body problem. The quantum aspect of an excess electron in molecular liquids is more and more captured by semiquantum molecular dynamics simulations or ab initio computations.⁴¹ In the specific cases of ultrafast electron attachment or solvation with sulfur-containing molecules, the analysis of quantum branchings needs to consider the structure of sulfur atomic core orbitals for ground and excited states.

Acknowledgment. This work is supported by GDR 1017 of the CNRS (France) and the Commission of the European Communities.

References and Notes

- (1) Lalitha, B.; Mittal, J. P. *Radiat. Eff.* **1971**, *7*, 159. Wolff, R. K.; Aldrich, J. E.; Penner, T. L.; Hunt, J. W. *J. Phys. Chem.* **1975**, *79*, 210. Bisby, R. H.; Cundall, R. B.; Redpath, J. L.; Adams, G. E. *J. Chem. Soc., Faraday Trans. 1* **1976**, *72*, 51.
- (2) *Sulfur-centered Reactive Intermediates in Chemistry and Biology*; Chatgililoglu, C., Asmus, K. D., Eds.; Plenum Press: New York, 1990.
- (3) Kosower, N. S.; Kosower, E. M. In *Free Radicals in Biology*; Pryor, W. A., Ed.; Academic Press: New York, 1976; Vol. II, p 55.
- (4) Adam, F. C.; Smith, G. E.; Elliot, A. J. *Can. J. Chem.* **1978**, *56*, 1856.
- (5) McDiarmid, R. *J. Chem. Phys.* **1974**, *61*, 274. Moran, S.; Ellison, B. *J. Phys. Chem.* **1988**, *92*, 1794.
- (6) Steadman, J.; Baer, T. *J. Chem. Phys.* **1988**, *89*, 5507. Tokue, I.; Hiraya, A.; Shobatake, K. *Chem. Phys.* **1989**, *130*, 401.
- (7) Effenhauser, C. S.; Felder, P.; Huber, J. R. *Chem. Phys.* **1990**, *142*, 311.
- (8) Appling, J. R.; Harbol, M. R.; Edgington, R. A. *J. Chem. Phys.* **1992**, *97*, 4041.
- (9) Thompson, S. D.; Carroll, D. G.; Watson, F.; O'Donnell, M.; McGlynn, S. P. *J. Chem. Phys.* **1966**, *45*, 1367.
- (10) Callear, A. B.; Dickson, D. R. *Trans. Faraday Soc.* **1970**, *7*, 1987.
- (11) Ohbayashi, K.; Akimoto, H.; Tanaka, I. *Chem. Phys. Lett.* **1977**, *52*, 47. Anastasi, C.; Broomfield, M.; Nielsen, O. J.; Pagsberg, P. *Chem. Phys. Lett.* **1991**, *182*, 643.
- (12) Asmus, K. D.; Bahnemann, D.; Fischer, C. H.; Veltwisch, D. *J. Am. Chem. Soc.* **1979**, *101*, 5322. Chaudri, A. A.; Göbl, M.; Freyholdt, T.; Asmus, K. D. *J. Am. Chem. Soc.* **1984**, *106*, 5988. Asmus, K. D. In *Sulfur-centered Reactive Intermediates in Chemistry and Biology*; Chatgililoglu, C., Asmus, K. D., Eds.; Plenum Press: New York, 1990; pp 155–172.
- (13) Baird, N. C. *J. Chem. Educ.* **1977**, *54*, 291.
- (14) Illies, A. J.; Livant, P.; McKee, M. L. *J. Am. Chem. Soc.* **1988**, *110*, 7980.
- (15) Clark, L. B.; Simpson, W. T. *J. Chem. Phys.* **1965**, *43*, 3666; Clark, T. *J. Am. Chem. Soc.* **1988**, *10*, 1672.
- (16) Marignier, J. L.; Belloni, J. *J. Phys. Chem.* **1981**, *85*, 310.
- (17) Hynes, A. J.; Wine, P. H.; Semmes, D. H. *J. Phys. Chem.* **1986**, *90*, 4148.
- (18) Charlson, R. J.; Lovelock, J. E.; Andreae, M. O.; Warren, S. G. *Nature* **1987**, *326*, 655.
- (19) Keene, W. C.; Pszenny, A. A. P.; Jacob, D. J.; Duce, R. A.; Galloway, J. N.; Schultz-Tokos, J. J.; Sievering, H.; Boatman, J. F. *Glob. Biogeochem. Cycles* **1990**, *4*, 407.
- (20) Bates, T. S.; Lamb, B. K.; Guenther, A.; Dignon, J.; Stoiber, R. E. *J. Atmos. Chem.* **1992**, *14*, 337.
- (21) Butkovskaya, N. I.; LeBras, G. *J. Phys. Chem.* **1994**, *98*, 2582.
- (22) Schöneich, C.; Bobrowski, K. *J. Phys. Chem.* **1994**, *98*, 12613.
- (23) Tyndall, G.; Ravishankara, A. R. *Int. J. Chem. Kinet.* **1991**, *23*, 483. Turnipseed, A. A.; Barone, S. B.; Ravishankara, A. R. *J. Phys. Chem.* **1992**, *96*, 7502.
- (24) Belloni, J.; Marignier, J. L.; Katsumura, Y.; Tabata, Y. *J. Phys. Chem.* **1986**, *90*, 4014.
- (25) Gauduel, Y.; Pommeret, S.; Antonetti, A.; Belloni, J.; Marignier, J. L. *J. Phys.* **1991**, *1*, 161.
- (26) Göbl, M.; Bonifacic, M.; Asmus, K. D. *J. Am. Chem. Soc.* **1984**, *106*, 5984.
- (27) Gauduel, Y. *J. Mol. Liq.* **1995**, *63*, 1. Gauduel, Y.; Gelabert, H.; Ashokkumar, M. *Chem. Phys.* **1995**, *197*, 167.
- (28) Cullen, W. R.; Frost, D. C.; Vroom, D. A. *Inorg. Chem.* **1969**, *8*, 1803. Cradock, S.; Whiteford, R. A. *J. Chem. Soc., Faraday Trans.* **1972**, *2*, 281.
- (29) Scott, J. D.; Causley, G. C.; Russel, B. R. *J. Chem. Phys.* **1973**, *59*, 6577.
- (30) Gauduel, Y.; Pommeret, S.; Yamada, N.; Migus, A.; Antonetti, A. *J. Am. Chem. Soc.* **1989**, *111*, 4974.
- (31) Goepfert-Mayer, M. *Ann. Phys.* **1931**, *9*, 273.
- (32) Karmann, W.; Granzow, A.; Meissner, G.; Heinglein, A. *Radiat. Phys. Chem.* **1969**, *1*, 395.
- (33) Gauduel, Y.; et al. In preparation.
- (34) Durig, J. R.; Griffin, M. G. *J. Chem. Phys.* **1977**, *67*, 2220; Durig, J. R.; Jalilian, M. R.; Sullivan, J. F.; Compton, D. A. *J. Chem. Phys.* **1981**, *75*, 4833.
- (35) Senent, M. L.; Moule, D. C.; Smeyers, Y. G. *J. Phys. Chem.* **1995**, *99*, 7970.
- (36) Nielsen, O.; Sidebottom, H. W.; Nelson, L.; Treacy, J. J.; O'Farrell, D. J. *Int. J. Chem. Kinet.* **1989**, *21*, 1101.
- (37) Stickel, R. E.; Nicovich, J. M.; Wang, S.; Zhao, Z.; Wine, P. H. *J. Phys. Chem.* **1992**, *96*, 9875.
- (38) McKee, M. L. *J. Phys. Chem.* **1993**, *97*, 10971.
- (39) Gu, M.; Turecek, F. *J. Am. Chem. Soc.* **1992**, *114*, 7146. Turecek, F. *J. Phys. Chem.* **1994**, *98*, 3701.
- (40) Barone, S. B.; Turnipseed, A. A.; Ravishankara, A. R. *J. Phys. Chem.* **1996**, *100*, 14694, 14703.
- (41) In *Ultrafast Reaction Dynamics and Solvent Effects*; Gauduel, Y., Rossky, P. J., Eds.; AIP Press: New York, 1994; Vol. 298. See also a recent Special Issue of *J. Chim. Phys.* **1996**, *93*, 1577–1938.